

# 1 NO<sub>3</sub> chemistry of wildfire emissions: a kinetic study of the gas-phase reactions of furans with the NO<sub>3</sub> radical

2 Mike J. Newland, Yangang Ren, Max R. McGillen, Lisa Michelat, Véronique Daële, Abdelwahid Mellouki

3 ICARE-CNRS, 1 C Av. de la Recherche Scientifique, 45071 Orléans Cedex 2, France

4  
5  
6 Correspondence to: Mike J. Newland ([mike.newland@cnrs-orleans.fr](mailto:mike.newland@cnrs-orleans.fr); [mellouki@cnrs-orleans.fr](mailto:mellouki@cnrs-orleans.fr))

7  
8  
9 **Abstract.** Furans are emitted to the atmosphere during biomass burning from the pyrolysis of cellulose. They are one of the  
10 major contributing VOC classes to OH and NO<sub>3</sub> reactivity in biomass burning plumes. The major removal process of furans  
11 from the atmosphere at night is reaction with the nitrate radical, NO<sub>3</sub>. Here we report a series of relative rate experiments in the  
12 7300 L indoor simulation chamber at CNRS-ICARE, Orléans, using a number of different reference compounds to determine  
13 NO<sub>3</sub> reaction rate coefficients for four furans, two furanones, and pyrrole. In the case of the two furanones, this is the first time  
14 that NO<sub>3</sub> rate coefficients have been reported. The recommended values (cm<sup>3</sup> molecule<sup>-1</sup> s<sup>-1</sup>) are: furan (1.49±0.23)×10<sup>-12</sup>, 2-  
15 methylfuran (2.26±0.52)×10<sup>-11</sup>, 2,5-dimethylfuran (1.02±0.31)×10<sup>-10</sup>, furfural (furan-2-aldehyde) (9.07±2.3)×10<sup>-14</sup>, α-  
16 angelicalactone (5-methyl-2(3H)-furanone) (3.01±0.45)×10<sup>-12</sup>, γ-crotonolactone (2(5H)-furanone) <1.4×10<sup>-16</sup>, and pyrrole  
17 (6.94±1.9)×10<sup>-11</sup>. The furfural + NO<sub>3</sub> reaction rate coefficient is found to be an order of magnitude smaller than previously  
18 reported. These experiments show that for furan, alkyl substituted furans, α-angelicalactone, and pyrrole, reaction with NO<sub>3</sub> will  
19 be the dominant removal process at night, and may also contribute during the day. For γ-crotonolactone, reaction with NO<sub>3</sub> is  
20 not an important atmospheric sink.

## 21 1 Introduction

22 Furans are five membered aromatic cyclic ethers. Furans (and pyrroles – where N replaces O as the heteroatom) are generated  
23 during the pyrolysis of cellulose and are a major component of emissions from wildfire burning (Hatch et al., 2015, 2017; Koss  
24 et al., 2018; Coggon et al., 2019; Andreae et al., 2019). Such emissions are likely to increase in the future with the spatial extent,  
25 number, and severity, of wildfires globally having increased markedly in recent decades (Jolly et al., 2015; Harvey, 2016) and  
26 predicted to continue to do so as the climate warms (Krikken et al., 2019; Lohmander, 2020). Furans have also been measured  
27 in emissions from residential logwood burning (Hartikainen et al., 2018), and burning of a wide variety of solid-fuels used for  
28 domestic heating and cooking (Stewart et al., 2021a). Furans have been shown to account for a significant proportion of the total  
29 NO<sub>3</sub> (Decker et al., 2019) and OH (Koss et al., 2018; Coggon et al., 2019; Stewart et al., 2021b) reactivity of emissions from  
30 burning of typical wildfire and domestic fuels.

31 Alkyl substituted furans have also been suggested as promising biofuels as they can be derived from lignocellulosic biomass  
32 (Roman-Leshkov et al., 2007; Binder et al., 2009; Wang et al., 2014). This would likely lead to fugitive emissions of these  
33 compounds during distribution, as well as emissions of unburned and partially oxidised products from vehicle exhaust. The  
34 oxidation of certain furan compounds has been shown to have large secondary organic aerosol yields (Hatch et al., 2017;  
35 Hartikainen et al., 2018; Joo et al., 2019; Ahern et al., 2019; Akherati et al., 2020), which could adversely impact air quality.

36 Oxidation of furans in the atmosphere has been shown to produce 2-furanones (mono-unsaturated five-membered cyclic esters)  
37 both via OH (notably hydroxy-furan-2-ones, Aschmann et al., 2014) and NO<sub>3</sub> (Berndt et al., 1997) reactions. 2-Furanones are

Deleted: 50
Deleted: 37
Deleted: 5
Deleted: 10
Deleted: 3
Deleted: 28
Deleted: 5-methyl-
Deleted: 0
Deleted: 2(5H)-furanone
Deleted: 7.35
Deleted: 2.06
Deleted: furan-2-aldehyde
Deleted: lower
Deleted: We also recommend a faster rate for the α-terpinene+NO <sub>3</sub> reaction ((2.70±0.81)×10 <sup>-10</sup> cm <sup>3</sup> s <sup>-1</sup> ).
Deleted: 5-methyl-2(3H)-furanone
Deleted: 2(5H)-furanone

55 also produced from the OH oxidation of six-membered aromatic compounds (Smith et al., 1998, 1999; Hamilton et al., 2005;  
56 Bloss et al., 2005; Wyche et al., 2009; Huang et al., 2015). In both cases, the initial product is thought to be an unsaturated  
57 dicarbonyl, with production of the 2-furanone formed via photoisomerisation of the dicarbonyl to a ketene-enol (Newland et al.,  
58 2019), followed by ring closure of this molecule. In the case of aromatics, the ketene-enol can also be formed directly via  
59 decomposition of the bicyclic peroxy radical intermediate (Wang et al., 2020).

60 Furan type compounds are removed from the atmosphere by reaction with the major oxidants OH, NO<sub>3</sub> and O<sub>3</sub>. There have been  
61 a number of studies on the rates of reaction of furan type compounds with the dominant daytime oxidant, OH (Lee and Tang,  
62 1982; Atkinson et al., 1983; Wine and Thompson, 1984; Bierbach et al., 1992, 1994, 1995; Aschmann et al., 2011; Ausmeel et  
63 al., 2017; Whelan et al., 2020). However, there have been fewer studies on the rates of reaction of furan type compounds with  
64 the major night-time oxidant, NO<sub>3</sub> (Atkinson et al., 1985; Kind et al., 1996; Cabañas et al., 2004; Colmenar et al., 2012).

65 The nitrate radical, NO<sub>3</sub>, is produced in the atmosphere predominantly through the reaction of NO<sub>2</sub> with O<sub>3</sub>, and exists in  
66 equilibrium with N<sub>2</sub>O<sub>5</sub>. It has long been known to be an important night-time oxidant (Levy, 1972; Winer et al., 1984). While it  
67 is also produced during the daytime, it is rapidly converted back to NO<sub>2</sub> by reaction with NO and by photolysis. However, in  
68 environments with low NO, either due to low NO<sub>x</sub> emissions, or suppression through high O<sub>3</sub> concentrations (e.g. Newland et  
69 al., 2021), NO<sub>3</sub> oxidation has been observed to be significant during the day (Hamilton et al., 2021).

70 Here, we present results of a series of relative rate experiments for furan, 2-methylfuran, 2,5-dimethylfuran, furfural (furan-2-  
71 aldehyde), α-angelicalactone (5-methyl-2(3H)-furanone), γ-crotonolactone (2(5H)-furanone), and pyrrole reaction with the NO<sub>3</sub>  
72 radical, performed in the 7300 L indoor simulation chamber at CNRS-ICARE, Orléans, France.

Deleted: (furfural

Deleted: (α-angelicalactone

Deleted: (γ-crotonolactone

## 73 2 Experimental

### 74 2.1 CSA-Chamber

75

76 The CNRS-ICARE indoor chamber is a 7300 L indoor simulation chamber used for studying reaction kinetics and mechanisms  
77 under atmospheric boundary layer conditions. Further details of the chamber setup and instrumentation are available elsewhere  
78 (Zhou et al., 2017). Experiments were performed in the dark at atmospheric pressure (*ca.* 1000 mbar), with the chamber operated  
79 at a slight overpressure to compensate for removal of air for sampling, and to prevent ingress of outside air to the chamber. The  
80 chamber is in a climate controlled room and the temperature was maintained at 299±2 K.

81

### 82 2.2 Experimental Approach

83

84 Starting with the chamber filled with clean air, the VOCs of interest (*ca.* 3 ppmv) were added, followed by ~ 1 Torr of the inert  
85 gas SF<sub>6</sub> to monitor the chamber dilution rate. The chamber was left for at least thirty minutes prior to the start of the experiment  
86 to monitor the dilution rate and losses of the VOCs to the chamber walls. These losses,  $(1 - 8) \times 10^{-6} \text{ s}^{-1}$ , were always smaller than  
87 dilution ( $\sim 1.2 \times 10^{-5} \text{ s}^{-1}$ ). The reaction was then initiated by continuously introducing an N<sub>2</sub>O<sub>3</sub> sample, held in a trap at ~ 235 K,  
88 with air flow of (2.5 – 5) L/min through it, for the duration of the experiment. The chamber was monitored until most of the  
89 VOC of interest was consumed, with experiments generally taking 0.5 – 2 hours. The experiments were performed under dry  
90 conditions (RH ≤ 1.5 %).

Deleted: continually

Deleted: ,

96 VOC abundance was determined by *in-situ* Fourier Transform Infrared (FTIR) Spectroscopy using a Nicolet 5700 coupled to a  
97 White-type multipass cell with a pathlength of 143 m. Each scan was comprised of either 30 or 60 co-additions, taking a total of  
98 2 or 4 minutes respectively, depending on the expected rate of loss of the VOCs, with a spectral resolution of 0.25 cm<sup>-1</sup>.

99

### 100 2.3 Materials

101

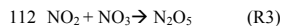
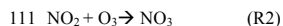
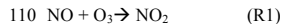
102 The VOCs of interest: furan (>99%, Sigma-Aldrich), 2-methylfuran (>98%, TCI), 2,5-dimethylfuran (>98%, TCI), pyrrole  
103 (>99%, TCI),  $\alpha$ -angelicalactone (>98%, TCI), furfural (>98%, TCI), and  $\gamma$ -crotonolactone (>93%, TCI); and reference  
104 compounds:  $\alpha$ -terpinene (90%, Sigma-Aldrich), 2,3-dimethyl-but-2-ene (98%, Sigma-Aldrich), 2-carene (97%, Sigma-Aldrich),  
105 camphene (95%, Sigma-Aldrich),  $\alpha$ -pinene (98%, Sigma-Aldrich), cyclohexene ( $\geq$ 99%, Sigma-Aldrich), 3-methyl-3-buten-1-ol  
106 (97%, Sigma-Aldrich), and cyclohexane (99.5%, Sigma-Aldrich), were used as supplied without further purification.

Deleted: Furan

107 N<sub>2</sub>O<sub>5</sub> was synthesised by reacting NO<sub>2</sub> with excess O<sub>3</sub>. First, NO and O<sub>3</sub> were mixed to generate NO<sub>2</sub> (Reaction R1). This NO<sub>2</sub> /  
108 O<sub>3</sub> mixture was then flushed into a bulb in which NO<sub>3</sub> and subsequently N<sub>2</sub>O<sub>5</sub> were generated through Reactions R2-R3.

Deleted: and  $\gamma$ -crotonolactone (>93%, TCI),

109



113

114 N<sub>2</sub>O<sub>5</sub> crystals were then collected in a cold trap at 190K. The N<sub>2</sub>O<sub>5</sub> sample was purified by trap to trap distillation under a flow  
115 of O<sub>2</sub> / O<sub>3</sub>. The final sample was stored at 190 K and used within a week.

116

### 117 2.4 Analysis

118

119 VOC concentrations were monitored by FTIR. The furans generally have a number of major absorption bands in the infrared.  
120 The main bands used for analysis are shown in Table 1 (bold), as well as other characteristic bands for each compound. Reference  
121 spectra of the major bands for each compound taken in the chamber at a resolution of 0.25 cm<sup>-1</sup> are provided in the Supplement  
122 (Figures S8-S14). The ANIR curve fitting software (Ródenas, 2018), which implements a least squares fitting algorithm was  
123 used to generate time profiles for each compound based on their reference spectra. Profiles were checked by doing a number of  
124 manual subtractions. Example time profiles from an experiment with  $\alpha$ -angelicalactone and furan, with cyclohexene as the  
125 reference compound, are shown in Figure 1. Further example plots are provided in the supplement (Figures S1-S7). All of the  
126 concentration-time profiles are provided in .txt format at 10.5281/zenodo.5721518, and all the raw FTIR output is provided in  
127 .csv format at 10.5281/zenodo.5721518. Relative rate plots for all of the experiments are shown in Figure 2.

Deleted: S1

Deleted: S7

Deleted: from

Deleted: with furan and 2-methylfuran

128

129

130

131

132

133

134

141 **Table 1** Maxima of major absorption bands (of Q branches if present) for the compounds used in this study. Bands used  
142 predominantly for analysis are shown in bold.

Compound	Main absorption bands / cm <sup>-1</sup>
Furan	<b>995</b> , 744
2-Methylfuran	<b>792</b> , 726, 1151, 2965
2,5-Dimethylfuran	777, 2938, 2961
Furfural	<b>756</b> , 1720
Pyrrrole	<b>724</b> , 1017, 3531, 718-722
<del><u>α-angelicalactone</u></del>	<b>731, 939</b> , 1100, 1834
<del><u>γ-crotonolactone</u></del>	<b>1098</b> , 805, 866, 1045, 1812, 2885, 2945
<del><u>2,3-Dimethyl-2-butene</u></del>	<b>2878, 2930, 3005</b>
<del><u>2-Carene</u></del>	<b>2874, 2928, 3009</b>
<del><u>α-pinene</u></del>	<b>2971, 2998, 3035, 789, 2847, 2893,</b> 2925, 2931
<del><u>Camphene</u></del>	<b>2967, 2972, 2986, 882, 2881, 3075</b>
<del><u>Cyclohexene</u></del>	<b>2934, 744, 919, 1140, 2892, 2943,</b> 3033, 3036
<del><u>3-Methyl-3-buten-1-ol</u></del>	<b>1065, 896, 903, 2886, 2948, 2981, 3084</b>
<del><u>Cyclohexane</u></del>	<b>2862, 2933</b>

143

144 Relative rate experiments were performed, whereby a compound (or two) with an unknown reaction rate coefficient ( $k_{VOC}$ ) with  
145 NO<sub>3</sub> was added to the chamber with a reference compound with a known NO<sub>3</sub> reaction rate coefficient ( $k_{ref}$ ). A plot of the relative  
146 loss of the compound against the reference compound following addition of NO<sub>3</sub> (via N<sub>2</sub>O<sub>5</sub> decomposition), accounting for both  
147 chamber dilution and wall losses ( $k_d$ ), gives a gradient of  $k_{VOC}/k_{ref}$  (Equation E1).

148

$$149 \ln \frac{([VOC]_0)}{([VOC]_t)} - k_d t = \frac{k_{VOC}}{k_{ref}} \ln \frac{[ref]_0}{[ref]_t} - k_d t \quad (E1)$$

150

151 A number of reference compounds were used for each VOC, chosen so that the reference rate coefficient was roughly within a  
152 factor of five of the expected unknown rate coefficient, and with an attempt to use different references that had both larger and  
153 smaller NO<sub>3</sub> reaction rate coefficients, than the VOC. Rate coefficients of the reference compounds (Table 2) are taken from the  
154 Database for the Kinetics of the Gas-Phase Atmospheric Reactions of Organic Compounds v2.1.0 (McGillen et al., 2020),  
155 available at [data.eurochamp.org/data-access/kin/#/home](http://data.eurochamp.org/data-access/kin/#/home).

156 N<sub>2</sub>O<sub>5</sub> was not present at detectable levels (by FTIR) during most of the experiments. The only experiments in which N<sub>2</sub>O<sub>5</sub>  
157 concentrations built up in the chamber, were those with the slowest reacting VOCs, i.e. furfural and γ-crotonolactone. NO<sub>2</sub>  
158 concentrations increased throughout all experiments, typically up to 2 – 3 ppmv. The NO<sub>2</sub> is initially produced from the  
159 decomposition of N<sub>2</sub>O<sub>5</sub>, and later potentially by the loss of NO<sub>2</sub> from nitrated VOCs / nitrated radicals. HNO<sub>3</sub> concentrations  
160 increased throughout the experiments, typically up to 3 – 4 ppmv. This could be either due to impurities in the N<sub>2</sub>O<sub>5</sub> sample, or

**Deleted:** S-Methyl-2(3H)-furanone

**Deleted:** 2(5H)-furanone

**Deleted:** faster

**Deleted:** slower

**Deleted:** s

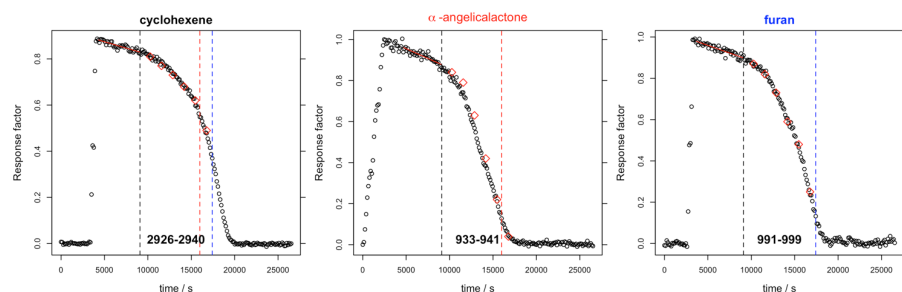
**Deleted:** Reaction r

**Deleted:** s

168 from H abstraction reactions of NO<sub>3</sub>. It is not thought that this level of HNO<sub>3</sub> will cause any interference in the rate coefficient

169 determinations.

170



171

172 **Figure 1** Concentration-time profiles from experiment with cyclohexene,  $\alpha$ -angelicalactone and furan. Black circles are response  
173 factors generated by the ANIR curve fitting program relative to the reference spectra. Red diamonds are obtained from manual  
174 subtractions. Left black dashed vertical line is the beginning of the region used for the relative rate calculation, the red dashed  
175 line is the end of the region used for the calculation of the  $\alpha$ -angelicalactone relative rate, the blue line is the end of the region  
176 used for the calculation of the furan relative rate. Bold values at the bottom are the absorption bands used for analysis.

177 **Table 2.** Reference compounds used. Recommended rate coefficients and uncertainties from McGillen et al. (2020).

Compound	$k / \text{cm}^3 \text{molecule}^{-1} \text{s}^{-1}$
2,3-dimethyl-2-butene	$(5.70 \pm 1.71) \times 10^{-11}$
2-carene	$(2.0 \pm 0.3) \times 10^{-11}$
$\alpha$ -pinene	$(6.20 \pm 1.55) \times 10^{-12}$
camphene	$(6.60 \pm 1.65) \times 10^{-13}$
cyclohexene	$(5.60 \pm 0.84) \times 10^{-13}$
3-methyl-3-buten-1-ol	$(2.60 \pm 0.78) \times 10^{-13}$
<u>cyclohexane</u>	<u><math>(1.35 \pm 0.20) \times 10^{-16}</math></u>

178

179 It is noted that no OH scavenger was used in these experiments (as is the case for most, if not all, NO<sub>3</sub> previous relative rate  
180 studies to the authors' knowledge). NO<sub>3</sub> reaction with alkenes tends to proceed by electrophilic addition to the double bond  
181 followed by addition of O<sub>2</sub> to the resulting radical, leading to a nitrooxy peroxy radical ( $\beta$ -ONO<sub>2</sub>-RO<sub>2</sub>) (Barnes et al., 1989;  
182 Hjorth et al., 1990). It has recently been shown (Novelli et al., 2021) that there is the possibility of OH formation through the  
183 reactions of  $\beta$ -ONO<sub>2</sub>-RO<sub>2</sub> with HO<sub>2</sub>. HO<sub>2</sub> could be generated in these experiments from the abstraction of an H atom by O<sub>2</sub> from  
184 a  $\beta$ -ONO<sub>2</sub>-RO radical with available H atoms. The initial NO<sub>3</sub> reaction with furans is not thought to form  $\beta$ -ONO<sub>2</sub>-RO<sub>2</sub> radicals,  
185 with NO<sub>3</sub> addition to the C2 carbon followed by O<sub>2</sub> addition to the C5 carbon (Berndt et al., 1997), analogous to the OH addition  
186 reaction (Bierbach et al., 1995; Mousavipour et al., 2009; Yuan et al., 2017; Whelan et al., 2020). However, some of the reference  
187 compounds used in the experiments will form such radicals. For example, the reaction of HO<sub>2</sub> with the  $\beta$ -ONO<sub>2</sub>-RO<sub>2</sub> radicals  
188 formed from  $\alpha$ -pinene + NO<sub>3</sub> has been reported to have an OH yield of up to 70 % (Kurtén et al., 2017). An additional minor

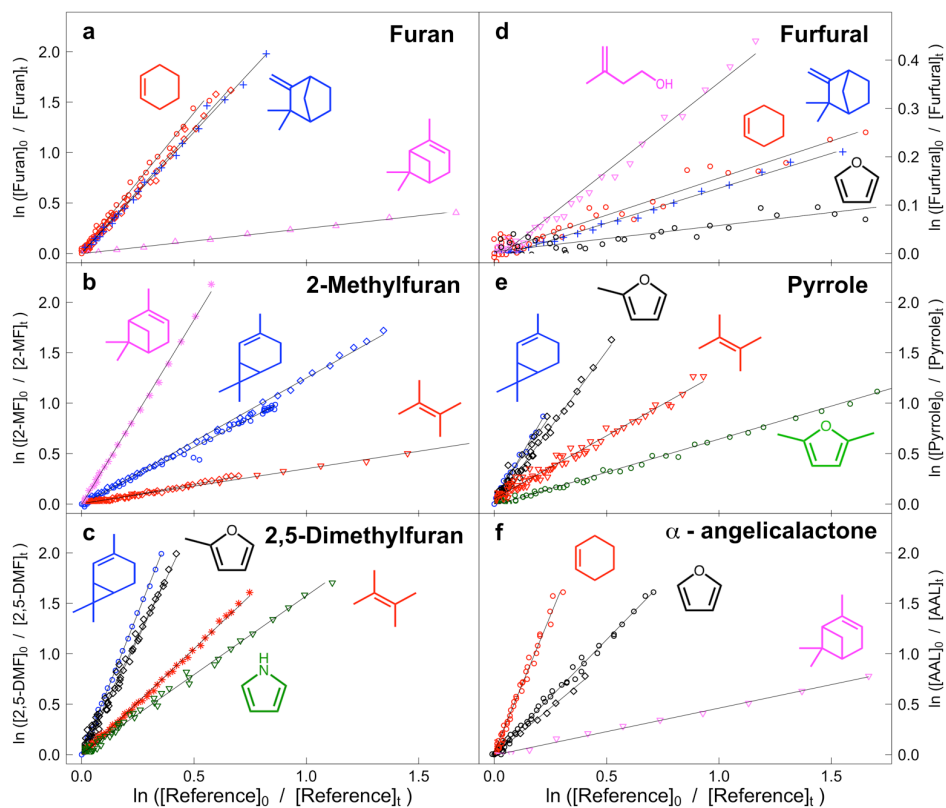
Deleted: s

Deleted: 6

191 source of HO<sub>2</sub> during the experiments will be H abstraction reactions by NO<sub>3</sub>. These will produce RO<sub>2</sub> that can react to form RO  
192 radicals which may yield HO<sub>2</sub> following abstraction of an H atom by O<sub>2</sub>. However, the rate coefficient of H abstraction by NO<sub>3</sub>  
193 is generally expected to be negligible relative to that of the NO<sub>3</sub> addition pathway. A box model run was performed to test the  
194 impact of this chemistry in this study. The  $\alpha$ -pinene scheme from the MCMv3.3.1 (Jenkin et al., 1997; mcm.york.ac.uk) was  
195 incorporated into the box model AtChem (Sommariva et al., 2020), and an OH yield of 0.5 was assigned to the reaction of HO<sub>2</sub>  
196 with the initial  $\beta$ -ONO<sub>2</sub>-RO<sub>2</sub> radicals formed from the  $\alpha$ -pinene+NO<sub>3</sub> reaction. The model was initiated with 2-methylfuran and  
197  $\alpha$ -pinene concentrations of 3 ppmv, representative of the experiments performed here. NO<sub>3</sub> concentrations were constrained to  
198 give a lifetime of  $\sim 1$  hour for the VOCs, typical of the experiments. OH reaction was found to account for less than 1 % of the  
199 removal of 2-methylfuran or  $\alpha$ -pinene through the model run. Consequently, it can be assumed that OH chemistry is a negligible  
200 interference in these experiments.

201 A further potential interference with the current experimental setup, is the reaction of NO<sub>2</sub> with the compounds used. Rate  
202 coefficients have been measured for reaction of NO<sub>2</sub> with a number of unsaturated compounds. For conjugated dienes, these  
203 values can be large enough ( $\sim 10^{-18}$  cm<sup>3</sup> molecule<sup>-1</sup> s<sup>-1</sup>) to provide a significant loss under the experimental conditions employed  
204 here (Atkinson et al., 1984; Bernard et al., 2013). NO<sub>2</sub> is formed during these experiments from the decomposition of N<sub>2</sub>O<sub>5</sub>, with  
205 the NO<sub>2</sub> mixing ratio typically increasing up to roughly 3 ppmv through the experiment. Separate experiments were performed  
206 to look at the potential reaction of NO<sub>2</sub> with furan, 2,5-dimethylfuran and pyrrole. For all three compounds, their loss in the  
207 presence of NO<sub>2</sub> (allowing for dilution) was indistinguishable from zero, allowing an upper limit of  $< 2 \times 10^{-20}$  cm<sup>3</sup> molecule<sup>-1</sup> s<sup>-1</sup>  
208 to be placed on their  $k(\text{NO}_2)$  rate coefficients.

209



210

211 **Figure 2.** Relative rate plots for: **a.** furan relative to cyclohexene (red), camphene (blue), and  $\alpha$ -pinene (pink); **b.** 2-methylfuran  
 212 relative to 2-carene (blue), 2,3-dimethyl-2-butene (red), and  $\alpha$ -pinene (pink); **c.** 2,5-dimethylfuran relative to 2-carene (blue),  
 213 2,3-dimethyl-2-butene (red), 2-methylfuran (black), and pyrrole (green); **d.** furfural relative to camphene (blue), cyclohexene  
 214 (red), furan (black), and 3-methyl-3-buten-1-ol (pink); **e.** pyrrole relative to 2-carene (blue), 2,3-dimethyl-2-butene (red), 2-  
 215 methylfuran (black), and 2,5-dimethylfuran (green); **f.**  $\alpha$ -angelicalactone relative to cyclohexene (red), furan (black), and  $\alpha$ -  
 216 pinene (pink). Different shapes are used for different experiments with the same reference compound.

### 217 3 Results and Discussion

218 The  $k(\text{NO}_3)$  rate coefficients determined with each reference compound are given in Table 3 and Figure 3. A recommendation  
 219 of an updated rate coefficient for  $\alpha$ -terpinene+ $\text{NO}_3$  is also given in Table 3. Overall recommended values for the rate coefficient  
 220 for each compound are calculated by taking the mean (weighted by the reported uncertainty of the reference) of the rate

Deleted:

Deleted:

223 coefficient derived from each experiment with each reference compound, including using the recommended values for the other  
224 furans presented in Table 3. Uncertainties for the relative rates in Table S1 are assumed to be < 10 % and to be dominated by  
225 statistical errors in fitting to the absorption bands. Uncertainties for the rate coefficients reported in Table 3 are dominated by  
226 the assumed uncertainties in  $k(\text{NO}_3)$  of the reference compounds. For most of the references, the uncertainties are 20 – 30 %,  
227 taken from the recommendations of McGillen et al. (2020). For 2,3-dimethyl-2-butene, the recommended uncertainty in  
228 McGillen et al. (2020) is 150 %, but based on the fact that the rate coefficients derived using 2,3-dimethyl-2-butene for 2-  
229 methylfuran, 2,5-dimethylfuran and pyrrole agree very well with those using other references with much smaller uncertainties,  
230 a conservative estimate of 30 % is used here. It is noted that for all compounds, the rate coefficients derived with different  
231 references agree very well, to within 10%. The experimentally determined  $k(\text{NO}_3)$  rate coefficients of the furans relative to each  
232 other are in good agreement (to within 6%) with those calculated using the weighted means shown in Table 3 (Table S2). This  
233 gives further confidence in the  $k(\text{NO}_3)$  values used for the reference compounds.

Deleted: and for  $\alpha$ -terpinene

234

235 The rate coefficient derived for furan, agrees well with the value previously reported by Atkinson et al. (1985) from a chamber  
236 relative rate experiment. However, there is significant differences between the values reported here for furan, 2-methylfuran and  
237 2,5-dimethylfuran, and those reported by Kind et al. (1996) from relative rate experiments in a flow reactor. While the value  
238 reported for 2-methylfuran agrees within the uncertainties between the two studies, the values for furan and 2,5-dimethylfuran  
239 are ~ 50 % and 100 % greater respectively. It is unclear what is behind this observed disparity; the good agreement between the  
240 two studies for the 2-methylfuran rate coefficient suggests that there is not a systematic difference between the experimental  
241 setups. For pyrrole, the rate coefficient determined here is about 50% faster than the value reported by Atkinson et al. (1985)  
242 from a chamber relative rate experiment using  $\text{N}_2\text{O}_5$  thermal decomposition. Cabañas et al. (2004) reported an upper limit of  
243  $<1.8 \times 10^{-10} \text{ cm}^3 \text{ molecule}^{-1} \text{ s}^{-1}$  (298K) using an absolute technique of fast flow discharge.

Deleted: , with the exception of  $\alpha$ -terpinene, which is discussed further below

Deleted: s

244 For 2-furaldehyde (furfural) +  $\text{NO}_3$ , the rate coefficient recommended here is an order of magnitude slower than the only  
245 previously reported values (Colmenar et al., 2012), derived from small chamber relative rate experiments with 2-methyl-2-butene  
246 and  $\alpha$ -pinene as references. The rate coefficient from Colmenar et al. (2012) is very similar to the reported rate coefficient for  
247 furan+ $\text{NO}_3$ . This is surprising, since the presence of a formyl group attached to a double bond is expected to be strongly  
248 deactivating with respect to addition to that bond, due to the electron withdrawing mesomeric effect of the  $-\text{C}(\text{O})\text{H}$  group  
249 (Kerdouci et al., 2014). This has also been observed for other electrophilic addition reactions, such as those with OH and  $\text{O}_3$   
250 (Kwok and Atkinson, 1995; McGillen et al, 2011; Jenkin et al., 2020). And while there is the possibility of H abstraction from  
251 the formyl group, which would increase the overall rate coefficient, such reactions are typically of the order of  $10^{-14} \text{ cm}^3 \text{ s}^{-1}$   
252 (Kerdouci et al., 2014), and hence would not be expected to compensate for the reduction in the contribution to the overall rate  
253 coefficient of the addition reaction.

Deleted: ed

254 For 5-methyl-(3H)-furan-2-one ( $\alpha$ -angelica lactone) +  $\text{NO}_3$  this is the first reported rate coefficient. For (5H)-furan-2-one ( $\gamma$ -  
255 crotonolactone), relative rate experiments with several reference compounds were attempted, with the slowest reacting of these  
256 being cyclohexane ( $k_{\text{NO}_3} = 1.4 \times 10^{-16} \text{ cm}^3 \text{ molecule}^{-1} \text{ s}^{-1}$ ). Roughly 10 % of the cyclohexane was removed in this experiment  
257 (accounting for loss by dilution), with no appreciable loss of  $\gamma$ -crotonolactone. We can therefore deduce that  $k(\gamma$ -  
258 crotonolactone+ $\text{NO}_3) \ll 1.4 \times 10^{-16} \text{ cm}^3 \text{ molecule}^{-1} \text{ s}^{-1}$ . Again, this is the first time a  $\text{NO}_3$  reaction rate coefficient has been  
259 measured for this compound. A comparison of the two furanones shows that 5-methyl-(3H)-furan-2-one reacts more than four  
260 orders of magnitude faster than (5H)-furan-2-one. This can be explained in part by the presence of a methyl group, which is seen

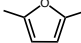
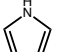
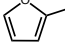
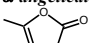
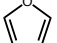
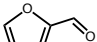
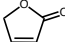


266 to increase the rate coefficient by roughly an order of magnitude from e.g. furan to 2-methylfuran to 2,5-dimethylfuran. Berndt  
 267 et al. (1997) derived an NO<sub>3</sub> reaction rate coefficient of 1.76×10<sup>-13</sup> cm<sup>3</sup> molecule<sup>-1</sup> s<sup>-1</sup> for (3H)-furan-2-one. However, the majority  
 268 of the difference must be explained by the structure of the two compounds, namely the conjugated nature of the C=C and C=O  
 269 bonds in (5H)-furan-2-one. The carbonyl group removes electron density from the C=C bond greatly reducing the rate  
 270 coefficient. A similar relationship is seen for analogous acyclic compounds e.g. the NO<sub>3</sub> rate coefficient of the conjugated ester  
 271 methyl acrylate is almost two orders of magnitude greater than that of the non-conjugated isomer vinyl acetate.

272

273

274 **Table 3.** NO<sub>3</sub> reaction rate coefficients derived for each experiment and recommended value based on the weighted mean.

Compound	Reference (repeats)	$k(\text{NO}_3) / \text{cm}^3 \text{ molecule}^{-1} \text{ s}^{-1}$	Weighted mean $k(\text{NO}_3) / \text{cm}^3 \text{ molecule}^{-1} \text{ s}^{-1}$
	2-carene (1)	1.12×10 <sup>-10</sup>	<del>1.02±0.31</del> ×10 <sup>-10</sup>
	2,3-dimethyl-2-butene (1)	1.21×10 <sup>-10</sup>	
	pyrrole (1)	<del>9.12</del> ×10 <sup>-10</sup>	
	2-methylfuran (2)	<del>9.06</del> ×10 <sup>-10</sup>	
	2-carene (1)	7.68×10 <sup>-11</sup>	<del>6.94±1.9</del> ×10 <sup>-11</sup>
	2,3-dimethyl-2-butene (2)	<del>7.07</del> ×10 <sup>-11</sup>	
	2,5-dimethylfuran (1)	<del>6.58</del> ×10 <sup>-11</sup>	
	2-methylfuran (2)	<del>6.37</del> ×10 <sup>-11</sup>	
	2-carene (3)	2.47×10 <sup>-11</sup>	<del>2.26±0.52</del> ×10 <sup>-11</sup>
	2,3-dimethyl-2-butene (2)	2.12×10 <sup>-11</sup>	
	α-pinene (1)	2.27×10 <sup>-11</sup>	
	pyrrole (2)	<del>1.89</del> ×10 <sup>-11</sup>	
	2,5-dimethylfuran (2)	<del>2.21</del> ×10 <sup>-11</sup>	
	α-pinene	<del>2.89</del> ×10 <sup>-12</sup>	<del>3.01±0.45</del> ×10 <sup>-12</sup>
	cyclohexene	<del>3.03</del> ×10 <sup>-12</sup>	
	furan (2)	3.05×10 <sup>-12</sup>	
	cyclohexene	<del>1.45</del> ×10 <sup>-12</sup>	<del>1.49±0.23</del> ×10 <sup>-12</sup>
	α-pinene	1.55×10 <sup>-12</sup>	
	camphene	1.58×10 <sup>-12</sup>	
	α-angelicalactone (2)	1.49×10 <sup>-12</sup>	
	cyclohexene (1)	<del>8.57</del> ×10 <sup>-14</sup>	<del>9.07±2.30</del> ×10 <sup>-14</sup>
	3-methyl-3-buten-1-ol (1)	9.54×10 <sup>-14</sup>	
	camphene (1)	9.50×10 <sup>-14</sup>	
	cyclohexane	< 1.4×10 <sup>-16</sup>	< 1.4×10 <sup>-16</sup>

Formatted: Width: 209.9 mm, Height: 274.8 mm, From text: 2 mm, Numbering: Continuous

Deleted: 10

Deleted: 3

Deleted: 1.10

Deleted: 1.07

Deleted: 7.35

Deleted: 2.06

Deleted: 6.87

Deleted: 7

Deleted: 22

Deleted: 7.52

Deleted: 37

Deleted: 5

Deleted: 2.28

Deleted: 4

Deleted: 3.03

Deleted: 0

Deleted: 2.89

Deleted: 46

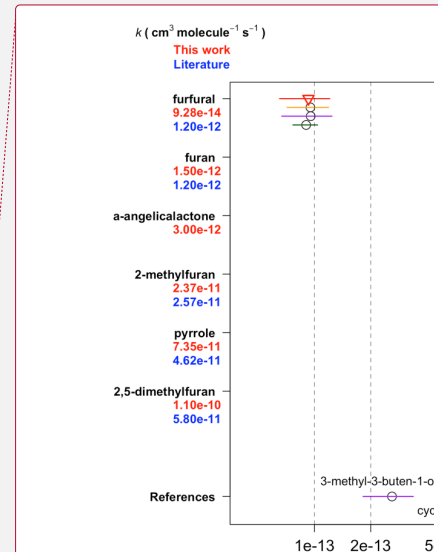
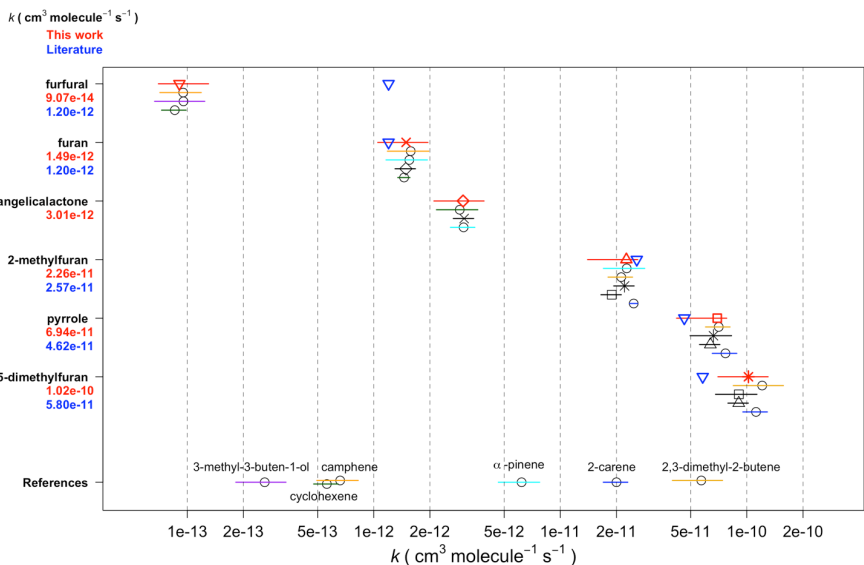
Deleted: 50

Deleted: 9.02

Deleted: 28

275

276



298  
 299 **Figure 3** The reaction rate coefficients derived for the six compounds in this work (excluding  $\gamma$ -crotonolactone). Red triangles  
 300 (and red text, left axis) represent the weighted mean of all experiments in this work, blue inverted triangles (and blue text, left  
 301 axis) are the recommended values from McGillen et al. (2020). Horizontal lines represent uncertainty in rate coefficient, colours  
 302 (shapes if other furans) represent which reference was used.

303  
 304  
 305 **Table 4.** Recommended  $\text{NO}_3$  rate coefficients from this work compared to those reported in the literature.

Compound	Rate coefficient / $\text{cm}^3 \text{ molecule}^{-1} \text{ s}^{-1}$	Reference	Technique	$\text{NO}_3$ source
<b>2,5-dimethylfuran</b>	<b><math>(1.02 \pm 0.31) \times 10^{-10}</math></b> $(5.78 \pm 0.34) \times 10^{-11}$	<b>This work</b> Kind et al. (1996)	Flow reactor: relative ( <i>trans</i> -2-butene)	$\text{N}_2\text{O}_5$
<b>pyrrole</b>	<b><math>(6.94 \pm 1.9) \times 10^{-11}</math></b> $(4.6 \pm 1.1) \times 10^{-11}$ $< 1 \times 10^{-10}$	<b>This work</b> Atkinson et al. (1985) Cabañas et al. (2004)	Chamber: relative (2-methyl-2-butene) Flow reactor: absolute (LIF detection of $\text{HNO}_3 + \text{FNO}_3$ )	$\text{N}_2\text{O}_5$ $\text{HNO}_3 + \text{FNO}_3$
<b>2-methylfuran</b>	<b><math>(2.26 \pm 0.52) \times 10^{-11}</math></b> $(2.57 \pm 0.17) \times 10^{-11}$	<b>This work</b> Kind et al. (1996)	Flow reactor: relative ( <i>trans</i> -2-butene)	$\text{N}_2\text{O}_5$
<b><math>\alpha</math>-angelicalactone</b>	<b><math>(3.01 \pm 0.45) \times 10^{-12}</math></b>	<b>This work</b>		
<b>furan</b>	<b><math>(1.49 \pm 0.23) \times 10^{-12}</math></b> $(1.5 \pm 0.2) \times 10^{-12}$ $(0.998 \pm 0.062) \times 10^{-12}$ $(1.36 \pm 0.8) \times 10^{-12}$	<b>This work</b> Atkinson et al. (1985) Kind et al. (1996) Cabañas et al. (2004)	Chamber: relative ( <i>trans</i> -2-butene) Flow reactor: relative ( <i>trans</i> -2-butene) Flow reactor: absolute (LIF detection of $\text{HNO}_3 + \text{FNO}_3$ )	$\text{N}_2\text{O}_5$ $\text{N}_2\text{O}_5$ $\text{HNO}_3 + \text{FNO}_3$

Deleted:  
 Formatted: Font:Bold

Deleted:  $\alpha$ -terpinene

Deleted: - [1]

Formatted: Width: 209.9 mm, Height: 274.8 mm, From text: 2 mm

Deleted:  $\alpha$ -terpinene [2]

Deleted: 10

Deleted: 3

Deleted: 2006

Deleted: 7.35

Deleted: 2.06

Deleted: 37

Deleted: 5

Deleted: 2006

Deleted: 00

Deleted: 50

Deleted: '

Deleted: 2006

<i>furfural</i>	$(9.07 \pm 2.30) \times 10^{-14}$ ( $1.17 \pm 0.15$ ) $\times 10^{-12}$	<b>This work</b> Colmenar et al. (2012)	Small chamber: relative (2-methyl-2-butene)	N <sub>2</sub> O <sub>5</sub>
	( $1.36 \pm 0.38$ ) $\times 10^{-12}$	Colmenar et al. (2012)	Small chamber: relative ( $\alpha$ -pinene)	N <sub>2</sub> O <sub>5</sub>
<i><math>\gamma</math>-crotonolactone</i>	$< 1.4 \times 10^{-16}$	<b>This work</b>		

Deleted: 28

<sup>a</sup> corrected for change to recommended rate for reference (2,3-dimethyl-2-butene); <sup>b</sup> corrected for change to recommended rate

Deleted: \*

323 for reference (trans-2-butene)

324

325

#### 326 4. Atmospheric implications

327

328 The atmospheric lifetimes of the compounds, based on the rate coefficients reported herein, are given in Table 5. These assume  
329 concentrations of OH =  $5 \times 10^6$  molecules cm<sup>-3</sup> (typical daily peak summertime concentrations  $1.5 \times 10^6 - 1.5 \times 10^7$  molecules cm<sup>-3</sup>  
330 (Stone et al., 2012)), night-time NO<sub>3</sub> =  $2 \times 10^8$  molecules cm<sup>-3</sup> (typical night-time concentrations  $1 \times 10^8 - > 1 \times 10^9$  cm<sup>-3</sup> (Brown  
331 and Stutz (2012)) daytime NO<sub>3</sub> =  $1 \times 10^7$  molecules cm<sup>-3</sup> (limited daytime measurements suggest concentrations ~ 0.5 - >1 pptv  
332 ( $2.5 \times 10^7$  molecules cm<sup>-3</sup>) (Brown and Stutz (2012)), and O<sub>3</sub> = 40 ppbv (background O<sub>3</sub> concentration ~ 40 ppb (Parrish et al.,  
333 2014)). From these values it is clear that the alkyl substituted furans and pyrrole have very short lifetimes both during the day,  
334 when the dominant daytime sink is likely to be reaction with OH, and at night, when the dominant sink will be reaction with  
335 NO<sub>3</sub>. O<sub>3</sub> may contribute somewhat to the removal of these compounds both during the day and night, particularly for 2,5-  
336 dimethylfuran. As  $k(\text{NO}_3)$  approaches the same order of magnitude as  $k(\text{OH})$ , e.g. for 2-methylfuran, 2,5-dimethylfuran and  
337 pyrrole, the NO<sub>3</sub> reaction is likely to be competitive with the OH reaction even during the day in low NO<sub>x</sub> environments, with  
338 daytime NO<sub>3</sub> concentrations reported to be ~ 1 ppt ( $2.5 \times 10^7$  molecules cm<sup>-3</sup>) (Brown and Stutz, 2012). The relatively large rate  
339 coefficient reported here for  *$\alpha$ -angelicalactone*, suggests that NO<sub>3</sub> reaction will be an important sink for unsaturated non-  
340 conjugated cyclic esters. On the other hand, the very small rate coefficient for the  *$\gamma$ -crotonolactone* + NO<sub>3</sub> reaction suggests that  
341 this will not be an important atmospheric sink.  *$\gamma$ -crotonolactone* has also been shown to have a very slow reaction with O<sub>3</sub>  
342 (lifetime > 100 years, Ausmeel et al., 2017), whereas for reaction with OH, the lifetime is much shorter, and this will be the  
343 predominant gas-phase sink for  *$\gamma$ -crotonolactone*. Such a slow NO<sub>3</sub> reaction might be expected to extend to all 2-furanones with  
344 a conjugated structure, e.g. hydroxyfuranones – major products of OH oxidation of methyl substituted furans (Aschmann et al.,  
345 2014), such that the nitrate reaction may be unimportant in the atmosphere for these structures. Although substitution at the  
346 double bond is likely to increase the rate coefficient somewhat, as observed for OH and O<sub>3</sub> reactions with the methyl-substituted  
347 form of  *$\gamma$ -crotonolactone* (Ausmeel et al., 2017).

Deleted: -

Moved up [1]: Atmospheric implications -

Moved (insertion) [1]

Deleted: 5-methyl-2(3H)-furanone

Deleted: slow

Deleted: of

Deleted: 2(5H)-furanone

Deleted: 2(5H)-furanone

Deleted: 2(5H)-furanone

Deleted: 2(5H)-furanone

348 One of the major sources of furan type compounds to the atmosphere is wildfires. Wildfire plumes can be regions of high NO<sub>3</sub>  
349 even during the day due to suppressed photolysis rates in optically thick plumes (Decker et al, 2021). NO<sub>3</sub> oxidation of furans  
350 may be even more important in such plumes than in the background atmosphere. Such plumes can extend over hundreds of  
351 kilometres and hence affect air quality on a local and regional scale (e.g. Andreae et al., 1988; Brocchi et al., 2018; Johnson et  
352 al., 2021). Domestic wood burning is an increasing trend in northern European cities (Chafe et al., 2015). Burning will generally  
353 be in the winter during which, with short daylight hours and peak daytime OH often an order of magnitude lower than during  
354 the summer, the reaction with NO<sub>3</sub> is likely to be the dominant fate of furan type compounds in such emissions, contributing  
355 significantly to organic aerosol in urban areas (Kodros et al., 2020).

367 Berndt et al. (1997) identified the major first generation products of furan+NO<sub>3</sub> to be the unsaturated dicarbonyl, butenedial, and  
 368 2(3H)-furanone, with the NO<sub>3</sub> recycled back to NO<sub>2</sub>. However, Tapia et al. (2011), and Joo et al. (2019) found that the major  
 369 products of the 3-methylfuran+NO<sub>3</sub> reaction predominantly retain the NO<sub>3</sub> functionality. In this case, furan+NO<sub>3</sub> oxidation  
 370 chemistry may be a significant sink for NOx, sequestering it in nitrate species, which might release it far from source on further  
 371 gas-phase oxidation, or, due to their low volatility, be taken up into aerosol (Joo et al. 2019).

Deleted: 6

372  
373  
374  
375  
376  
377  
378  
379  
380  
381  
382

383 **Table 5.** Atmospheric gas-phase lifetimes of the compounds reported herein based on typical mid-day OH concentrations of  
 384  $5 \times 10^6$  molecules cm<sup>-3</sup>, night-time NO<sub>3</sub> concentrations of  $2 \times 10^8$  molecules cm<sup>-3</sup>, day-time NO<sub>3</sub> concentrations of  $1 \times 10^7$  molecules  
 385 cm<sup>-3</sup>, and background O<sub>3</sub> concentrations of 40 ppbv ( $1 \times 10^{12}$  molecules cm<sup>-3</sup>).

Compound	$\tau_{\text{NO}_3}$ (night)	$\tau_{\text{NO}_3}$ (day)	$\tau_{\text{OH}}$ (day)	$\tau_{\text{O}_3}$	$\tau_{\text{total}}$ (day)
2,5-dimethylfuran	0.82 min	16 min	26 min <sup>a</sup>	40 min <sup>b</sup>	8 min
2-methylfuran	3.7 min	74 min	48 min <sup>a</sup>	-	28 min
furan	56 min	19 hours	83 min <sup>a</sup>	116 hours <sup>c</sup>	77 min
pyrrole	1.2 min	24 min	28 min <sup>d</sup>	18 hours <sup>d</sup>	13 mins
furfural	15 hours	13 days	95 min <sup>e</sup>	-	94 min
$\alpha$ -angelicalactone	28 min	9.3 hours	48 min <sup>f</sup>	3.5 hours <sup>g</sup>	37 mins
$\gamma$ -crotonolactone	> 1.1 year	> 22 years	14 hours <sup>h</sup>	173 years	14 hours

Deleted: 76

Deleted: 15

Deleted: 5

Deleted: 70

Deleted: 1

Deleted: 23

Deleted: 2

Deleted: 5-methyl-2(3H)-furanone

Deleted: 2(5H)-furanone

386 <sup>a</sup>Matsumoto (2011), <sup>b</sup>Dillon et al. (2012); <sup>c</sup>Atkinson et al. (1983); <sup>d</sup>Atkinson et al. (1984); <sup>e</sup>Bierbach et al. (1995); <sup>f</sup>Bierbach  
 387 et al. (1994); <sup>g</sup>estimated (Bierbach et al., 1994); <sup>h</sup>Ausmeel et al. (2017)

388

## 389 5. Conclusions

Deleted: 4

390 Rate coefficients are recommended for reaction of seven furan type VOCs with NO<sub>3</sub> at 298 K and 760 Torr, based on a series of  
 391 relative rate experiments. These new recommendations highlight the importance of NO<sub>3</sub> chemistry to the removal of furans, and  
 392 other similar VOCs, under atmospheric conditions. The measured rate coefficients suggest that for the three furans reported here,  
 393 as well as for pyrrole and  $\alpha$ -angelicalactone, reaction with NO<sub>3</sub> is likely to be their dominant night-time sink. For the alkyl furans

Deleted: 5-methyl-2(3H)-furanone

406 and pyrrole, reaction with NO<sub>3</sub> may also be a significant sink during the daytime. This work also extends the existing database  
407 of VOC+NO<sub>3</sub> reactions, providing valuable reference values for future work.

408

409

410 *Data availability.* Further example plots and experiment information are provided in the supplement. All of the response-time  
411 profiles from the FTIR are provided in .txt format at [10.5281/zenodo.5724967](https://doi.org/10.5281/zenodo.5724967), and all of the raw FTIR output is provided in .csv  
412 format at [10.5281/zenodo.5721518](https://doi.org/10.5281/zenodo.5721518).

413

414 *Author contributions.* MJN performed the experiments with the technical support of YR and MRM and performed the data  
415 treatment and interpretation. MJN wrote the paper. All co-authors revised the content of the original manuscript and approved  
416 the final version of the paper.

417

418 *Competing interests.*

419 The authors declare that they have no conflict of interest.

420

421 *Special issue statement.* This article is part of the special issue “Simulation chambers as tools in atmospheric research  
422 (AMT/ACP/GMD inter-journal SI)”. It is not associated with a conference.

423

424 *Acknowledgements.*

425 This work is supported by the European Union’s Horizon 2020 research and innovation program through the EUROCHAMP-  
426 2020 Infrastructure Activity under grant agreement no. 730997, Labex Voltaire (ANR-10-LABX-100-01) and ANR (SEA\_M  
427 project, ANR-16-CE01-0013, program ANR-RGC 2016).

428

429 Financial support. This research has been supported by the European Commission Horizon 2020 Framework Programme (grant  
430 no. EUROCHAMP-2020 (730997)) and the Agence Nationale de la Recherche (grants nos. ANR-10-LABX-100-01 and ANR-  
431 16-CE01-0013)

## 432 References

433 Ahern, A. T., Robinson, E. S., Tkacik, D. S., Saleh, R., Hatch, L. E., Barsanti, K. C., Stockwell, C. E., Yokelson, R. J., Presto,  
434 A. A., Robinson, A. L., Sullivan, R. C., and Donahue, N. M.: Production of Secondary Organic Aerosol During Aging of Biomass  
435 Burning Smoke From Fresh Fuels and Its Relationship to VOC Precursors, *J. Geophys. Res.-Atmos.*, 124, 3583–3606, 2019.

436

437 Akherati, A., He, Y., Coggon, M. M., Koss, A. R., Hodshire, A. L., Sekimoto, K., Warneke, C., de Gouw, J., Yee, L., Seinfeld,  
438 J. H., Onasch, T. B., Herndon, S. C., Knighton, W. B., Cappa, C. D., Kleeman, M. J., Lim, C. Y., Kroll, J. H., Pierce, J. R., and  
439 Jathar, S. H.: Oxygenated Aromatic Compounds are Important Precursors of Secondary Organic Aerosol in Biomass Burning  
440 Emissions, *Environ. Sci. Technol.*, 54, 8568–8579, <https://doi.org/10.1021/acs.est.0c01345>, 2020.

441

442 Andreae, M. O., Browell, E. V., Garstang, M., Gregory, G. L., Harriss, R. C., Hill, G. F., Jacob, D. J., Pereira, C., Sachse, G.  
443 W., Setzer, A. W., Silva Dias, P. L., Talbot, R. W., Torres, A. L., and Wofsy, S. C.: Biomass-burning emissions and associated  
444 haze layers over Amazonia, *J. Geophys. Res.-Atmos.*, 93, 1509-1527, 1988.

**Deleted:** In addition to the rates for the furan type compounds, an updated recommendation is provided for *k*( $\alpha$ -terpinene+NO<sub>3</sub>), a reaction of particular importance as one of the fastest known VOC+NO<sub>3</sub> reaction rate coefficients.

**Deleted:** All relevant data and supporting information have been provided in the Supplement.

**Formatted:** Not Highlight

451  
452 Andreae, M. O.: Emission of trace gases and aerosols from biomass burning – an updated assessment, *Atmos. Chem. Phys.*, 19,  
453 8523–8546, <https://doi.org/10.5194/acp-19-8523-2019>, 2019.

454  
455 Aschmann, S. M., Nishino, N., Arey J., and Atkinson, R.: Products of the OH radical-initiated reactions of furan, 2- and 3-  
456 methylfuran, and 2,3- and 2,5-dimethylfuran in the presence of NO, *J. Phys. Chem. A*, 118, 457-466, 2014.

457  
458 Atkinson, R., Aschmann, S. M., and Carter, W. P. L.: Kinetics of the reactions of O<sub>3</sub> and OH radicals with furan and thiophene  
459 at 298 +/- 2 K, *Int. J. Chem. Kinet.*, 15, 51-61, 1983.

460  
461 Atkinson, R., Aschmann, S. M., Winer, A. M., and Carter, W. P. L.: Rate Constants for the Gas Phase Reactions of OH Radicals  
462 and O<sub>3</sub> with Pyrrole at 295 +/- 1 K and Atmospheric Pressure, *Atmos. Environ.*, 18, 2105-2107, 1984.

463  
464 [Atkinson, R., Aschmann, S. M., Winer, A. M., and Pitts, J. N.: Gas-phase reactions of NO<sub>2</sub> with alkenes and dialkenes, \*Int. J.\*  
465 \*Chem. Kinet.\*, 16, 697-706, 1984.](#)

466  
467 Atkinson, R., Aschmann, S. M., Winer, A. M., and Carter, W. P. L.: Rate Constants for the Gas Phase Reactions of NO<sub>3</sub> Radicals  
468 with Furan, Thiophene and Pyrrole at 295 +/- 1 K and Atmospheric Pressure, *Environ. Sci. Technol.*, 19, 87-90, 1985.

469  
470 Ausmeel, S., Andersen, C., Nielsen, O. J., Østerstrøm, F. F., Johnson, M. S., and Nilsson, E. J. K.: Reactions of Three Lactones  
471 with Cl, OD, and O<sub>3</sub>: Atmospheric Impact and Trends in Furan Reactivity, *J. Phys. Chem. A*, 121, 4123-4131, 2017.

472  
473 Barnes, I., Bastian, V., Becker, K. H., and Tong, Z.: Kinetics and products of the reactions of nitrate radical with monoalkenes,  
474 dialkenes, and monoterpenes, *J. Phys. Chem.*, 94, 2413–2419, 1990.

475  
476 [Bernard, F., Cazaunau, M., Mu, Y., Wang, X., Daële, V., Chen, J., and Mellouki, A.: Reaction of NO<sub>2</sub> with conjugated alkenes,  
477 \*J. Phys. Chem. A\*, 117, 14132-14140, 2013.](#)

478  
479 [Berndt, T., Böge, O., Kind, I., and Rolle, W.: Reaction of NO<sub>3</sub> Radicals with 1,3-cyclohexadiene,  \$\alpha\$ -terpinene, and  \$\alpha\$ -  
480 phellandrene, \*Ber. Bunsenges. Phys. Chem.\*, 100, 462–469, 1996.](#)

481  
482 Berndt, T., Böge, O., and Rolle, W.: Products of the Gas-Phase Reactions of NO<sub>3</sub> Radicals with Furan and Tetramethylfuran,  
483 *Environ. Sci. Technol.*, 31, 1157–1162, 1997.

484  
485 Bierbach, A., Barnes, I., Becker, K. H., and Wiesen, E.: Atmospheric Chemistry of Unsaturated Carbonyls: Butenedial, 4-Oxo-  
486 2-pentenal, 3-Hexene-2,5-dione, Maleic Anhydride, 3H-Furan-2-one, and 5-Methyl-3H-furan-2-one, *Environ. Sci. Technol.*, 28,  
487 715-729, 1994.

488  
489 Bierbach, A., Barnes, I., and Becker, K. H.: Product and kinetic study of the OH-initiated gas-phase oxidation of furan, 2-  
490 methylfuran and furanaldehydes at  $\approx$  300 K, *Atmos. Environ.*, 29, 2651–2660, 1995.

491  
492 Binder, J. B., and Raines, R. T.: Simple Chemical Transformation of Lignocellulosic Biomass into Furans for Fuels and  
493 Chemicals. *J. Am. Chem. Soc.*, 131, 1979–1985, 2009.

494  
495 Bloss, C., Wagner, V., Jenkin, M. E., Volkamer, R., Bloss, W. J., Lee, J. D., Heard, D. E., Wirtz, K., Martin-Reviejo, M., Rea,  
496 G., Wenger, J. C., and Pilling, M. J.: Development of a detailed chemical mechanism (MCMv3.1) for the atmospheric oxidation  
497 of aromatic hydrocarbons, *Atmos. Chem. Phys.*, 5, 641–664, <https://doi.org/10.5194/acp-5-641-2005>, 2005.

498  
499 Brocchi, V., Krysztofiak, G., Catoire, V., Guth, J., Marécal, V., Zbinden, R., El Amraoui, L., Dulac, F., and Ricaud, P.:

500 Intercontinental transport of biomass burning pollutants over the Mediterranean Basin during the summer 2014 ChArMEX-  
501 GLAM airborne campaign, *Atmos. Chem. Phys.*, 18, pp. 6887-6906, 2018.  
502  
503 Brown, S., and Stutz, J.: Nighttime radical observations and chemistry, *Chem. Soc. Rev.*, 41, 6405-6447, 2012.  
504  
505 Cabañas, B., Baeza, M. T., Salgado, S., Martín, P., Taccone, R., and Martínez, E.: Oxidation of heterocycles in the atmosphere:  
506 Kinetic study of their reactions with NO<sub>3</sub> radical, *J. Phys. Chem. A*, 108, 10818-10823, 2004.  
507  
508 Chafé, Z., Brauer, M., Héroux, M. -E., Klimont, Z., Lanki, T., Salonen, R. O., and Smith, K. R.: Residential heating with wood  
509 and coal: health impacts and policy options in Europe and North America, WHO Regional Office for  
510 Europe. <https://apps.who.int/iris/handle/10665/153671>, 2015.  
511  
512 Coggon, M. M., Lim, C. Y., Koss, A. R., Sekimoto, K., Yuan, B., Gilman, J. B., Hagan, D. H., Selimovic, V., Zarzana, K. J.,  
513 Brown, S. S., M Roberts, J., Müller, M., Yokelson, R., Wisthaler, A., Krechmer, J. E., Jimenez, J. L., Cappa, C., Kroll, J. H., De  
514 Gouw, J. and Warneke, C.: OH chemistry of non-methane organic gases (NMOGs) emitted from laboratory and ambient biomass  
515 burning smoke: Evaluating the influence of furans and oxygenated aromatics on ozone and secondary NMOG formation, *Atmos.*  
516 *Chem. Phys.*, 19, 14875–14899, doi:10.5194/acp-19-14875-2019, 2019.  
517  
518 Colmenar, I., Cabañas, B., Martínez, E., Salgado, M. S., and Martín, P.: Atmospheric fate of a series of furanaldehydes by their  
519 NO<sub>3</sub> reactions, *Atmos. Environ.*, 54, 177-184, 2012.  
520  
521 Decker, Z. C. J., Zarzana, K. J., Coggon, M., Min, K.-E., Pollack, I., Ryerson, T. B., Peischl, J., Edwards, P., Dubé, W. P.,  
522 Markovic, M. Z., Roberts, J. M., Veres, P. R., Graus, M., Warneke, C., de Gouw, J., Hatch, L. E., Barsanti, K. C. and Brown, S.  
523 S.: Nighttime Chemical Transformation in Biomass Burning Plumes: A Box Model Analysis Initialized with Aircraft  
524 Observations, *Environ. Sci. Technol.*, 53, 2529–2538, doi:10.1021/acs.est.8b05359, 2019.  
525  
526 Dillon, T. J., Tucceri, M. E., Dulitz, K., Horowitz, A., Vereecken, L., and Crowley, J.: Reaction of Hydroxyl Radicals with  
527 C<sub>4</sub>H<sub>5</sub>N (Pyrrole): Temperature and Pressure Dependent Rate Coefficients, *J. Phys. Chem. A*, 116, 6051-6058, 2012.  
528  
529 Fouqueau, A., Cirtog, M., Cazaunau, M., Pangui, E., Doussin J. -F., and Picquet-Varrault, B.: A comparative and experimental  
530 study of the reactivity with nitrate radical of two terpenes:  $\alpha$ -terpinene and  $\gamma$ -terpinene, *Atmos. Chem. Phys.*, 20, 15167-15189,  
531 2020.  
532  
533 Harvey B. J.: Human-caused climate change is now a key driver of forest fire activity in the western United States, *Proc. Natl.*  
534 *Acad. Sci.*, 113, 11649-11650, 2016.  
535  
536 Hartikainen, A., Yli-Pirilä, P., Tiitta, P., Leskinen, A., Kortelainen, M., Orasche, J., Schnelle-Kreis, J., Lehtinen, K.,  
537 Zimmermann, R., Jokiniemi, J., and Sippula, O.: Volatile Organic Compounds from Logwood Combustion: Emissions and  
538 Transformation under Dark and Photochemical Aging Conditions in a Smog Chamber, *Environ. Sci. Technol.*, 52, 4979-4988,  
539 2018.  
540  
541 Hatch, L. E., Luo, W., Pankow, J. F., Yokelson, R. J., Stockwell, C. E., and Barsanti, K. C.: Identification and quantification of  
542 gaseous organic compounds emitted from biomass burning using two-dimensional gas chromatography–time-of-flight mass  
543 spectrometry, *Atmos. Chem. Phys.*, 15, 1865–1899, <https://doi.org/10.5194/acp-15-1865-2015>, 2015.  
544  
545 Hatch, L. E., Yokelson, R. J., Stockwell, C. E., Veres, P. R., Simpson, I. J., Blake, D. R., Orlando, J. J., and Barsanti, K. C.:  
546 Multi-instrument comparison and compilation of non-methane organic gas emissions from biomass burning and implications for  
547 smoke-derived secondary organic aerosol precursors, *Atmos. Chem. Phys.*, 17, 1471–1489, 2017.  
548

549 Hjorth, J., Lohse, C., Nielsen, C. J., Skov, H., and Restelli, G.: Products and mechanism of the gas-phase reaction between  
550 NO<sub>3</sub> and a series of alkenes, *J. Phys. Chem.*, 94, 7494–7500, 1990.  
551

552 Jenkin, M. E., Saunders, S. M., and Pilling, M. J.: The tropospheric degradation of volatile organic compounds: a protocol for  
553 mechanism development, *Atmos. Environ.*, 31, 81–104, [https://doi.org/10.1016/S1352-2310\(96\)00105-7](https://doi.org/10.1016/S1352-2310(96)00105-7), 1997 (data available  
554 at: <http://mcm.york.ac.uk>, last access: 12 August 2021).  
555

556 Jenkin, M. E., Valorso, R., Aumont, B., Newland, M. J., and Rickard, A. R.: Estimation of rate coefficients for the reactions of  
557 O<sub>3</sub> with unsaturated organic compounds for use in automated mechanism construction, *Atmos. Chem. Phys.*, 20, 12921–12937,  
558 <https://doi.org/10.5194/acp-20-12921-2020>, 2020.  
559

560 Johnson, M. S., Strawbridge, K., Knowland, K. E., Keller, C., and Travis, M.: Long-range transport of Siberian biomass burning  
561 emissions to North America during FIREX-AQ, *Atmos. Environ.*, 252, 118241, 2021  
562

563 Jolly, W. M., Cochrane, M. A., Freeborn, P. H., Holden, Z. A., Brown, T. J., Williamson, G. J., and Bowman, D. M. J. S.:  
564 Climate-induced variations in global wildfire danger from 1979 to 2013, *Nat. Commun.*, 6, 7537, 2015.  
565

566 Kerdouci, J., Picquet-Varrault, B., and Doussin, J. -F.: Structure activity relationship for the gas-phase reactions of NO<sub>3</sub> radical  
567 with organic compounds: Update and extension to aldehydes, *Atmos. Environ.*, 84, 363-372, 2014.  
568

569 Kind, I., Berndt, T., Böge, O., and Rolle, W.: Gas-phase rate constants for the reaction of NO<sub>3</sub> radicals with furan and methyl-  
570 substituted furans, *Chem. Phys. Lett.*, 256, 679-683, 1996.  
571

572 Kodros, J., Papanastasiou, D., Paglione, M., Masiol, M. and Squizzato, S.: Rapid dark aging of biomass burning as an overlooked  
573 source of oxidized organic aerosol, 117, 33028-33033, 2020.  
574

575 Koss, A. R., Sekimoto, K., Gilman, J. B., Selimovic, V., Coggon, M. M., Zarzana, K. J., Yuan, B., Lerner, B. M., Brown, S. S.,  
576 Jimenez, J. L., Krechmer, J., Roberts, J. M., Warneke, C., Yokelson, R. J., and de Gouw, J.: Non-methane organic gas emissions  
577 from biomass burning: identification, quantification, and emission factors from PTR-ToF during the FIREX 2016 laboratory  
578 experiment, *Atmos. Chem. Phys.*, 18, 3299–3319, <https://doi.org/10.5194/acp-18-3299-2018>, 2018.  
579

580 Krikken, F., Lehner, F., Hausteiner, K., Drobyshev, I., and van Oldenborgh, G. J.: Attribution of the role of climate change in the  
581 forest fires in Sweden 2018, *Nat. Hazards Earth Syst. Sci.*, 21, 2169–2179, <https://doi.org/10.5194/nhess-21-2169-2021>, 2021.  
582

583 Kurtén, T., Möller, K. H., Nguyen, T. B., Schwantes, R. H., Misztal, P. K., Su, L., Wennberg, P. O., Fry J. L., and Kjaergaard,  
584 H. G.: Alkoxy Radical Bond Scissions Explain the Anomalously Low Secondary Organic Aerosol and Organonitrate Yields  
585 From alpha-Pinene + NO<sub>3</sub>, *J. Phys. Chem. Lett.*, 8, 2826–2834, 2017.  
586

587 Kwok, E. S. C., and Atkinson, R.: Estimation of hydroxyl radical reaction rate constants for gas-phase organic compounds using  
588 a structure-reactivity relationship: An update, *Atmos. Environ.*, 29, 1685-1695, 10.1016/1352-2310(95)00069-b, 1995.  
589

590 Lohmander, P.: Forest fire expansion under global warming conditions: Multivariate estimation, function properties, and  
591 predictions for 29 countries, *Central Asian Journal of Environmental Science and Technology Innovation*, 5, 262-276, 2020.  
592

593 Matsumoto, J.: Kinetics of the reactions of ozone with 2,5-dimethylfuran and its atmospheric implications, *Chem. Lett.*, 40, 582-  
594 583, 2011.  
595

596 McGillen, M. R., Archibald, A. T., Carey, T., Leather, K. E., Shallcross, D. E., Wenger, J. C., and Percival, C. J.: Structure-  
597 activity relationship (SAR) for the prediction of gas-phase ozonolysis rate coefficients: an extension towards heteroatomic  
598 unsaturated species, *Phys. Chem. Chem. Phys.*, 13, 2842-2849, 2011.



- 600 McGillen, M. R., Carter, W. P. L., Mellouki, A., Orlando, J. J., Picquet-Varrault, B., and Wallington, T. J.: Database for the  
601 kinetics of the gas-phase atmospheric reactions of organic compounds, *Earth Syst. Sci. Data*, 12, 1203–1216,  
602 <https://doi.org/10.5194/essd-12-1203-2020>, 2020.
- 603
- 604 Newland, M. J., Rea, G. J., Thüner, L. P., Henderson, A. P., Golding, B. T., Rickard, A. R., Barnes, I., and Wenger, J.:  
605 Photochemistry of 2-butenedial and 4-oxo-2-pentenal under atmospheric boundary layer conditions, *Phys. Chem. Chem. Phys.*,  
606 21, 1160–1171, 2019.
- 607
- 608 Novelli, A., Cho, C., Fuchs, H., Hofzumahaus, A., Rohrer, F., Tillmann, R., Kiendler-Scharr, A., Wahner, A., and Vereecken,  
609 L.: Experimental and theoretical study on the impact of a nitrate group on the chemistry of alkoxy radicals, 23, 5474–5495, 2021.
- 610
- 611 Parrish, D. D., Lamarque, J. F., Naik, V., Horowitz, L., Shindell, D. T., Staehelin, J., Derwent, R., Cooper, O. R., Tanimoto, H.,  
612 Volz-Thomas, A., Gilge, S., Scheel, H. E., Steinbacher, M. and Fröhlich, M.: Long-term changes in lower tropospheric baseline  
613 ozone concentrations: Comparing chemistry-climate models and observations at northern midlatitudes, *J. Geophys. Res.*, 119,  
614 5719–5736, doi:10.1002/2013JD021435, 2014.
- 615
- 616 Ródenas, M: software for analysis of Infrared spectra. EUROCHAMP-2020 project, 2018. Available at  
617 <https://data.eurochamp.org/anisoft>
- 618
- 619 Roman-Leshkov, Y., Barrett, C. J., Liu, Z. Y., and Dumesic, J. A.: Production of Dimethylfuran for Liquid Fuels from Biomass-  
620 derived Carbohydrates, *Nature*, 447, 982–985, 2007.
- 621
- 622 Smith, D. F., McIver, C. D., and Kleindienst, T. E.: Primary product distribution from the reaction of hydroxyl radicals with  
623 toluene at ppb NO<sub>x</sub> mixing ratios, *J. Atmos. Chem.*, 30, 209–228, 1998.
- 624
- 625 Smith, D. F., Kleindienst, T. E., and McIver, C. D.: Primary Product Distributions from the Reaction of OH with m-, p-Xylene,  
626 1,2,4- and 1,3,5-Trimethylbenzene, *J. Atmos. Chem.*, 34, 339–364, 1999.
- 627
- 628 Sommariva, R., Cox, S., Martin, C., Borońska, K., Young, J., Jimack, P. K., Pilling, M. J., Matthaios, V. N., Nelson, B. S.,  
629 Newland, M. J., Panagi, M., Bloss, W. J., Monks, P. S., and Rickard, A. R.: AtChem (version 1), an open-source box model for  
630 the Master Chemical Mechanism, *Geosci. Model Dev.*, 13, 169–183, <https://doi.org/10.5194/gmd-13-169-2020>, 2020.
- 631
- 632 Stewart, G. J., Acton, W. J. F., Nelson, B. S., Vaughan, A. R., Hopkins, J. R., Arya, R., Mondal, A., Jangirh, R., Ahlawat, S.,  
633 Yadav, L., Sharma, S. K., Dunmore, R. E., Yunus, S. S. M., Hewitt, C. N., Nemitz, E., Mullinger, N., Gadi, R., Sahu, L. K.,  
634 Tripathi, N., Rickard, A. R., Lee, J. D., Mandal, T. K., and Hamilton, J. F.: Emissions of non-methane volatile organic compounds  
635 from combustion of domestic fuels in Delhi, India, *Atmos. Chem. Phys.*, 21, 2383–2406, [https://doi.org/10.5194/acp-21-2383-](https://doi.org/10.5194/acp-21-2383-636)  
636 2021, 2021a.
- 637
- 638 Stewart, G. J., Nelson, B. S., Acton, W. J. F., Vaughan, A. R., Hopkins, J. R., Yunus, S. S. M., Hewitt, C. N., Nemitz, E.,  
639 Mullinger, N., Gadi, R., Rickard, A. R., Lee, J. D., Mandal, T. K., and Hamilton, J. F.: Comprehensive organic emission profiles,  
640 secondary organic aerosol production potential, and OH reactivity of domestic fuel combustion in Delhi, India, *Environ. Sci.:*  
641 *Atmos.*, <https://doi.org/10.1039/D0EA00009D>, online first, 2021b.
- 642
- 643 Stone, D., Whalley, L., and Heard, D.: Tropospheric OH and HO<sub>2</sub> radicals: field measurements and model comparisons, *Chem.*  
644 *Soc. Rev.*, 41, 6348–6404, 2012.
- 645
- 646 Wang, J. J., Liu, X. H., Hu, B. C., Lu, G. Z., Wang, Y. Q.: Efficient Catalytic Conversion of Lignocellulosic Biomass into  
647 Renewable Liquid Biofuels via Furan Derivatives. *RSC Adv.*, 4, 31101–31107, 2014.
- 648

649 Whelan, C. A., Eble, J. Mir, Z. S., Blitz, M. A., Seakins, P. W., Olzmann, M., and Stone D.: Kinetics of the Reactions of Hydroxyl  
650 Radicals with Furan and Its Alkylated Derivatives 2-Methyl Furan and 2,5-Dimethyl Furan, *J. Phys. Chem. A*, 124, 7416–7426,  
651 2020.

652

653 Wyche, K. P., Monks, P. S., Ellis, A. M., Cordell, R. L., Parker, A. E., Whyte, C., Metzger, A., Dommen, J., Duplissy, J., Prevot,  
654 A. S. H., Baltensperger, U., Rickard, A. R., and Wulfert, F.: Gas phase precursors to anthropogenic secondary organic aerosol:  
655 detailed observations of 1,3,5-trimethylbenzene photooxidation, *Atmos. Chem. Phys.*, 9, 635–665, [https://doi.org/10.5194/acp-](https://doi.org/10.5194/acp-9-635-2009)  
656 [9-635-2009](https://doi.org/10.5194/acp-9-635-2009), 2009.

657

658 Yuan, Y. Zhao, X., Wang, S., and Wang, L: Atmospheric Oxidation of Furan and Methyl-Substituted Furans Initiated by  
659 Hydroxyl Radicals, *J. Phys. Chem. A*, 121, 9306-9319, 2017.

$\alpha$ -terpinene was used as a reference compound in two experiments. However, the rate coefficients derived for 2,5-dimethylfuran and pyrrole are significantly smaller using  $\alpha$ -terpinene compared to other reference compounds. In addition, its reaction rate relative to 2,3-dimethyl-2-butene is larger than expected based on the recommended rate coefficient of  $(1.80\pm 1.44)\times 10^{-10}$  cm<sup>3</sup> molecule<sup>-1</sup> s<sup>-1</sup> (McGillen et al., 2020). The reaction with  $\alpha$ -terpinene is one of the largest known VOC+NO<sub>3</sub> rate coefficients, and hence it is a useful reference and important to know the rate with a good degree of certainty. We derive a rate coefficient relative to 2,5-dimethylfuran of 2.68, to pyrrole of 3.79 and to 2,3-dimethyl-2-butene of 4.39. Using the recommended values given in Table 3 for 2,5-dimethylfuran and pyrrole, and the recommended value for 2,3-dimethyl-2-butene in Table 2, gives an average NO<sub>3</sub> reaction rate for  $\alpha$ -terpinene of  $(2.70\pm 0.81)\times 10^{-10}$  cm<sup>3</sup> molecule<sup>-1</sup> s<sup>-1</sup>. This is considerably faster than a recent absolute rate measurement of  $(1.2\pm 0.3)\times 10^{-10}$  cm<sup>3</sup> molecule<sup>-1</sup> s<sup>-1</sup> (Fouqueau et al., 2020), and previous relative rate determinations of  $(1.6\pm 0.6)\times 10^{-10}$  cm<sup>3</sup> molecule<sup>-1</sup> s<sup>-1</sup> (Atkinson et al., 1985) and  $(0.9\pm 0.4)\times 10^{-10}$  (Berndt et al., 1996) using TME as a reference.

<i><math>\alpha</math>-terpinene</i>	$(2.74\pm 0.81)\times 10^{-10}$	<b>This work</b>	
	$(1.6\pm 0.6)\times 10^{-10}$	Atkinson et al. (1985)	Relative (2,3-dimethyl-2-butene)
	$(0.9\pm 0.4)\times 10^{-10}$	Berndt et al. (1996)	Relative (2,3-dimethyl-2-butene)
	$(1.2\pm 0.3)\times 10^{-10}$	Fouqueau et al. (2020)	